Brazilian Journal
of Chemical
Engineering

ISSN 0104-6632
Printed in Brazil
www.abeq.org.br/bjche

Vol. 31, No. 04, pp. 895 - 903, October - December, 2014
dx.doi.org/10.1590/0104-6632.20140314s00002895

EFFECT OF INTERNAL RECIRCULATION VELOCITY IN AN ANAEROBIC SEQUENCING BATCH REACTOR (ASBR)

G. Z. Maurina[1*], L. M. Rosa[1], L. L. Beal[1], C. Baldasso[1], J. R. Gimenez[1], A. P. Torres[2] and M. P. Sousa[2]

[1]Laboratory of Environmental Technology, University of Caxias do Sul,
1130 Franciso Getúlio Vargas st., Caxias do Sul - RS, Brazil.
Phone: + (55) (54) 3218 2100
E-mail: gzmaurin@ucs.br
[2]Cenpes, Petrobras, 950 Horácio Macedo Avenue, Rio de Janeiro - RJ, Brazil.

(Submitted: August 14, 2013 ; Revised: October 30, 2013 ; Accepted: November 13, 2013)

Abstract - This paper discusses the effect of different internal recirculation velocities on the mixture and shear stress on the flocs in an anaerobic sequencing batch reactor (ASBR). Thus, simulations are performed using a computational fluid dynamics (CFD) tool to evaluate this dependency. The analysis of velocities and turbulent kinetic energy indicates that the highest flow evaluated (0.003 m³/s) results in better mixing within the reactor. However, care must be taken with the recycling pipe size, in order to maintain the shear stress inside the range of optimal values.
Keywords: Computational fluid dynamics; Anaerobic processes; Anaerobic sequencing batch reactor.

INTRODUCTION

Currently, anaerobic processes have experienced a very significant development. They are a low cost technology and can be applied in processes such as wastewater treatment, production of biogas and biohydrogen.

One of the most used system is the anaerobic sequencing batch reactor (ASBR), which has been widely studied since the early nineties (Fernandes *et al.*, 1993; Brito *et al.*, 1997; Arooj *et al.*, 2007; Kim *et al.*, 2008).

The operation of an ASBR takes place in a single tank and comprises the following steps: (i) filling with wastewater; (ii) treatment by means of biotransformations of the wastewater constituents by microbial activity; (iii) settling of the biological sludge after reaction termination; (iv) discharge of the reactor (Pinheiro *et al.*, 2008; Michelan *et al.*, 2009). Most of the operation time is spent in step (ii), when the liquid is continuously recirculated to promote agitation. This sequence is repeated for each new batch.

Many are the variables that affect the performance of ASBRs, such as agitation, initial ratio between substrate and biomass concentrations, geometric configuration of the reactor, temperature and feeding strategy (Novaes *et al.*, 2010). Special attention should be given to agitation, especially in large scale applications, since it improves mass transfer and therefore increases the substrate consumption rate, which may reduce the total cycle length. Agitation is important not only to provide good mixing conditions (homogenization, improved contact between biomass and liquid medium) or increase mass transfer, but also to improve the solubilization of particulate organic matter, which may increase overall conversion and substrate consumption rates (Pinho *et al.*, 2005).

*To whom correspondence should be addressed

There are several ways to provide agitation in these systems, including recirculation of biogas, liquid recirculation and mechanical stirring. Mixing is usually accomplished in ASBRs by mechanical agitation or by recirculation of the biogas generated in the process (Michelan *et al.*, 2009). However, Brito *et al.* (1997) and Pinheiro *et al.* (2008) established that biogas production may be insufficient to promote the turbulence that is required to minimize both the occurrence of possible stagnant zones and mass transfer resistance. Thus, Brito *et al.* (1997) developed an ASBR where agitation was accomplished by recirculation of the effluent by means of a diaphragm pump, and concluded that it is possible to use effluent recirculation as a means of agitation. Pinheiro *et al.* (2008) evaluated the optimum recirculation velocity for an ASBR used in wastewater treatment, and found that the system is limited by mass transfer when operating with lower velocities.

However, higher velocities might reduce microbial activity due to excessive shearing, which may damage the flocs present in the biomass (Michelan *et al.*, 2009) and cause granule rupture, resulting in poor solid separation (Bannari *et al.*, 2011). From an engineering point of view, the hydrodynamic shear force, as a governing parameter, can be manipulated to enhance the active sludge granulation process for wastewater treatment (Ren *et al.*, 2009).

To study the influence of different forces on the fluid dynamics, many researchers have turned to computational fluid dynamics (CFD). The advancement of computer performance in the last decades has enabled the prediction of flow fields and improved mixing performance in anaerobic digesters. Ding *et al.* (2010) presented three-dimensional CFD simulations of a gas-liquid two-phase flow agitated by a mechanical impeller in a lab-scale continuous stirred-tank reactor (CSTR) for biohydrogen production. It has been shown that the impeller type and speed significantly affect flow patterns: the relation between hydrodynamics and biohydrogen production indicated that an impeller operating at speeds between 50 and 70 rpm provided better reactor performance. Wang *et al.* (2010) introduced the CFD methodology developed by Ding *et al.* (2010) into the investigation of scale-up mechanisms for the CSTR, and indicated that parameters such as velocity field and stagnation zone needed to be optimized in industrial-scale reactors. Yu *et al.* (2013) associated the multi-fluid model with the Kinetic Theory of Granular Flow (KTGF) and Anaerobic Digestion Model no.1 (ADM1) to improve the performance of an anaerobic digester, where settling and suspension are very important phenomena to retain biomass.

In this context, the aim of this work is to employ CFD techniques to study the effect of liquid recirculation velocity on the performance and stability of an ASBR. The modeling method developed and the results of this study should provide a better understanding of the mixing inside the reactor, which can improve momentum and mass transfer, and aid in finding a good balance between mass transfer and shear stress distributions.

METHODOLOGY

Reactor Configuration and Operational Conditions

The reactor studied in this work consists of a pilot scale ASBR used to produce biohydrogen, located currently in an industrial plant in Campinas, Brazil. It has an internal diameter of 0.604 m, height of 3.8 m and a total capacity of 1.0 m^3. As the initial condition, the ASBR is considered to be filled with wastewater and biogas. The simulation starts with the liquid recycle, which promotes agitation in the bioreactor. The recycling pipe has an internal diameter of 0.04 m. A diagram of the reactor is shown in Figure 1. In the experimental setup, a pipe is placed at the top, and is used to withdraw the produced biogas. In the simulations presented here, fermentation reactions are not considered, thus gas is not produced and this region was treated as a wall. The recycle pipe was replaced by inlet and outlet conditions.

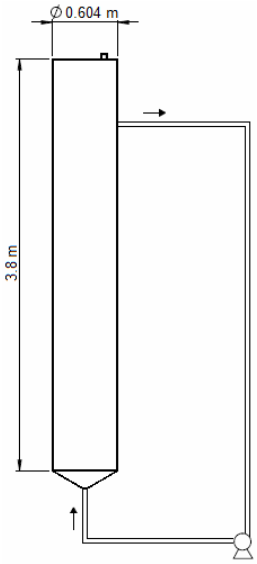

Figure 1: Schematic diagram of the ASBR studied.

The reactor studied currently operates with a recycle flow rate of 0.0015 $m^3.s^{-1}$. In order to verify

the effect of the flow rate increase on the efficiency of mixing, three cases with different operational conditions were initially considered. The flow rates adopted were 0.0015, 0.00225 and 0.0030 $m^3.s^{-1}$, corresponding to 1, 1.5 and 2 times the original condition. The Newtonian fluid adopted for simulations has rheological properties similar to the mixture of microbial culture and substrate composed of vinasse and glycerin, discarded respectively in conventional alcohol plants and biodiesel units. The gas phase has the properties of biogas.

Mathematical Modeling

Simulations were conducted with the OpenFOAM CFD toolbox. The solver used to carry out the simulations adopts the Eulerian-Eulerian approach, which is also referred to as the two-fluid model, where both phases are treated as interpenetrating fluids. The ensemble-average mass and momentum conservation equations are used to describe the time-dependent motion of both phases. Averaged interaction terms describing the interfacial forces appear in the momentum balance of both phases. The phases are composed of (1) a continuous liquid mixture, and (2) gas bubbles. Gas is expected to be present only in the top section of the reactor, with the presence of bubbles only at the interface between fluid and gas.

The formulation described by Weller (2002) *apud* Rusche (2002) for incompressible two-phase flow is adopted. In this formulation, the momentum equation of the phase is divided by the respective volume fraction, to avoid the singularity that may occur at the limit of one phase fraction approaching zero. The balance equations for continuity and intensive momentum can be written using Equations (1) and (2):

$$\frac{\partial}{\partial t}\left(\alpha_g\right)+\nabla\left(\alpha_g U\right)+\nabla\left(U_r\alpha_g\left(1-\alpha_g\right)\right)=0 \tag{1}$$

$$\frac{\partial}{\partial t}\left(U_i\right)+U_i.\nabla\left(U_i\right)+\nabla.\left(R_i^{eff}\right)+\frac{\nabla\alpha_i}{(\alpha_i+\delta)}.R_i^{eff}= -\frac{\nabla p}{\rho_i}+g+\frac{M_i}{(\alpha_i+\delta)\rho_i} \tag{2}$$

where the *i* subscript indicates the phase, liquid (*l*) or gas (*g*). U and α represent the velocity vector and the phase fraction. δ is a small value (0.001), applied to avoid zero division errors which could arise in the absence of one phase $\left(\alpha_i=0\right)$. The term R_i^{eff} represents the combined Reynolds (turbulent) and viscous stress, as defined in Equation (3):

$$R_i^{eff}=-\upsilon_i^{eff}\left(\nabla U_i+\nabla U_i^T-\frac{2}{3}I\nabla.U_i\right)+\frac{2}{3}Ik_i=0 \tag{3}$$

where υ_i^{eff} is the effective viscosity of the phase, I is the unit tensor, and k is the turbulent kinetic energy.

In Equation (2), M_i represents the momentum transferred due to the sum of interfacial forces. According to Chen *et al.* (2005) and Silva *et al.* (2012), gas-liquid flows in bubble columns are dominated by the drag force and, if it is modeled correctly, the drag force can establish the flow pattern without the addiction of other interfacial forces. In the present study, the interaction between gas bubbles and liquid is due only to the interface of liquid and gas phases. Thus, forces such as lift, virtual mass and turbulent dispersion have a minimum effect on the flow, and the drag force should be sufficient to describe the gas-liquid interaction. M_i is expressed according to Equation (4):

$$M_g=-M_l=\frac{3}{4}\frac{\alpha_g\rho_l}{d_g}C_D\left|U_r\right|U_r \tag{4}$$

where U_r is the relative velocity between the phases, d_g represents the bubble diameter, and C_D is the drag coefficient, obtained using the Schiller and Naumann correlation (Equation (5)):

$$C_D=\begin{cases}\frac{24}{\mathrm{Re}}\left(1+0.15\mathrm{Re}^{0.687}\right) & \text{when Re} \le 1000\\ \left(0.44\right) & \text{when Re} \ge 1000\end{cases} \tag{5}$$

where Re denotes the bubble Reynolds number, defined in Equation (6):

$$\mathrm{Re}=\frac{\left|U_r\right|d_g}{\upsilon_l} \tag{6}$$

The *k-epsilon* turbulence model was used to determine the effects of turbulence in the liquid phase. The effective viscosity of the continuous phase is given by the sum of the laminar viscosity υ_l and the eddy viscosity υ^t, which is calculated with Equation (7):

$$\upsilon^t=C_\mu\left(k^2/\varepsilon\right) \tag{7}$$

Conservative equations for *k* and *epsilon* are presented in Equations (8) and (9), respectively:

$$\frac{\partial}{\partial t}(k_l)+(U_l.\nabla)k_l-\nabla.\left(\frac{\upsilon_l^{eff}}{\sigma_k}\nabla k_l\right)=P_k-\varepsilon_l \quad (8)$$

$$\frac{\partial}{\partial t}(\varepsilon_l)+(U_l.\nabla)\varepsilon_l-\nabla.\left(\frac{\upsilon_l^{eff}}{\sigma_\varepsilon}\nabla\varepsilon_l\right)=\frac{\varepsilon_l}{k_l}(C_1P_k-C_2\varepsilon_l) \quad (9)$$

where P_k is the production of turbulent kinetic energy, obtained using Equation (10):

$$P_k=2\upsilon_l^{eff}\left(\nabla U_l.dev\left(\nabla U_l+(\nabla U_l)^T\right)\right) \quad (10)$$

The values used for the coefficients of the *k-epsilon* model are shown in Table 1.

Table 1: Coefficients used in the *k-epsilon* model.

C_μ	C_1	C_2	σ_k	σ_ε
0.09	1.44	1.92	1.0	0.76923

Numerical Solution and Boundary Conditions

OpenFOAM solvers use the finite volume method to solve systems of partial differential equations applied to any 3D unstructured mesh of polyhedral cells. New solvers and utilities can be created with the knowledge of the underlying method, physics and programming techniques involved (Bannari *et al.*, 2008). The simulations carried out in this work available in version 2.2.1 of OpenFOAM. This solver uses a comprehensive list of interpolation schemes. In this work, linear Gaussian integration for gradient operators was chosen. It is based on summing values on cell faces, which must be interpolated from cell centers. A Gauss linear scheme, which interpolates variables based on fluxes, was used for discretization of divergence terms. For the first time derivative, the choice was the Euler implicit first order technique (Rusche, 2002; OpenFOAM, 2013). The solution of the resulting equations is made with the segregated technique, solving each set of algebraic equations separately within an iterative cycle with an appropriate solver until convergence is achieved. A special treatment is required in order to establish the necessary inter-equation coupling, thus the solution of the pressure equation provides corrections for updating pressure, flux and velocities, satisfying the continuity criterion.

The numerical solution is based on a mix between the SIMPLE and PISO algorithms to handle the pressure-velocity coupling. It involves a momentum predictor and a correction loop in which a pressure equation based on the volumetric continuity equation is solved, and the momentum is corrected based on the pressure change (Rusche, 2002). Iterative methods are used to solve the system of algebraic equations created by discretization of partial differential equations. The generalized "Geometric-Algebraic Multi-Grid" (GAMG) solver was used to solve for the pressure with tolerance equal to 1×10-8, "Preconditioned Bi-Conjugate Gradient" (PBiCG) was used to solve for the dissipation and turbulent kinetic energy, with tolerance equal to 1×10-5, and "Preconditioned Conjugated Gradient" (PCG) was used to solve for the phase fraction with tolerance equal to 1×10-10.

To guarantee temporal accuracy and numerical stability, a Courant-Friedrichs-Lewy (CFL) condition of less than one was applied, avoiding the need of use relaxation factors. This resulted in variable time steps for the transient simulations, mostly under 10-3 s. They were processed in parallel, using four cores in a Z600 HP workstation. Each simulation had 300 s of flow calculated, with the last 100 s used to obtain average values.

With a three-dimensional geometry of the reactor, automatic meshes were generated using the "snappyHexMesh" software. They were composed predominantly of hexahedral volumes, with polyhedral elements to adjust the volumes close to the geometry surfaces. Seven meshes were evaluated, with approximately 60,000, 90,000, 130,000, 150,000, 170,000, 190,000 and 210,000 control volumes. The results of pressure and velocity in multiphase simulations were used as mesh evaluation criteria, in order to determine the optimal mesh size to carry out this study. It was found that 130,000 control volumes are sufficient to correctly estimate the flow in this reactor. This mesh is illustrated in Figures 2A and 2B. It has y+ values (dimensionless measure of the thickness of the control volumes adjacent to the walls of the reactor) approximately equal to 37, which is suitable for turbulent cases simulations.

The feed is composed of the liquid mixture, without bubbles. Thus, the interaction between the phases is present only at the interface, close to 3.68 m height. The bubble diameter was set to 0.001 m (Ding *et al.*, 2010) with the assumption of spherical bubbles. Table 2 shows the boundary conditions and physical properties used in the cases proposed.

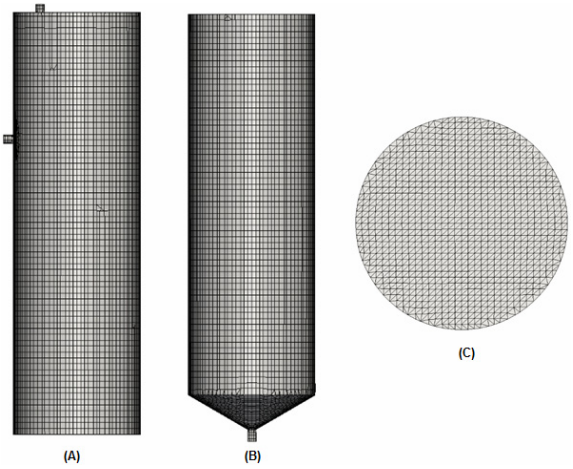

Figure 2: Details of the mesh used: (A) superior section and (B) inferior section at the walls; and (C) transversal cut.

Table 2: Boundary conditions and physical properties used in the numerical simulations.

Boundary Conditions		
Inlet	Case 1: flow rate of 0.0015 $m^3.s^{-1}$ Case 2: flow rate of 0.00225 $m^3.s^{-1}$ Case 3: flow rate of 0.0030 $m^3.s^{-1}$	
Outlet	101,325 Pa	
Walls	Smooth surface, non-slipping condition for both phases	
Physical Properties		
Phase	**Density**	**Kinematic viscosity**
Disperse (gas)	0.089 $kg.m^{-3}$	8.4×10^{-6} $m^2.s^{-1}$
Continuous (liquid)	1,009.7 $kg.m^{-3}$	1×10^{-6} $m^2.s^{-1}$
Bubbles diameter	0.001 m	

The boundary conditions for *k* and *epsilon* at the inlet were calculated using Equations (11) and (12), respectively:

$$k = \frac{3}{2}\left(0.05U_{l,inlet}\right)^2 \quad (11)$$

$$\varepsilon = C_{\mu}^{3/4}\frac{k^{3/2}}{0.2L} \quad (12)$$

where 0.05 represents the turbulence intensity at the inlet (5%), and *L* the characteristic length, depending on the inlet diameter.

Shear Stress Determination

As already mentioned, the shear stress is an important parameter affecting bioreactors, as it strongly influences the floc morphology, and thus the activity of microorganisms. The maximal shear stress in each control volume is evaluated using Equation (13), proposed by Bannari *et al.* (2011):

$$\tau_{\max} = \mu_{eff}.\max\left(\left|\tau_{xy}\right|,\left|\tau_{xz}\right|,\left|\tau_{yz}\right|,\left|\tau_{xx}\right|,\left|\tau_{yy}\right|,\left|\tau_{zz}\right|\right) \quad (13)$$

RESULTS AND DISCUSSION

Three cases are initially presented, considering different flow rates. The average results obtained for Case 1, with a flow rate of 0.0015 $m^3.s^{-1}$, are shown in Figure 3. This figure shows planes that cut the reactor along its height. It can be noted in Figure 3A that most of the liquid phase mixing speed of the liquid phase is maintained below 0.3 m/s and the maximal speed (1.5 $m.s^{-1}$) is found in the lower portion of the reactor, at the inlet pipe.

The flow inside the reactor shows no preferential paths, as can be seen in Figure 3B. The velocity vectors in this figure were normalized to better show the presence of large vortices. There are no vectors at the top, as the reactor is filled with gas in this region. The lower speeds inside the reactor, associated with the analysis of turbulent kinetic energy (Figure 3C), indicates the existence of areas with low mixing, mainly located in the top portion of the reactor.

Figure 4 shows the results obtained for Case 2, considering the recycle flow of 0.00225 $m^3.s^{-1}$. Comparing Figures 3A and 4A, it can be seen that the increase of 50% in the flow rate causes an overall increase in the mixing rate of the liquid phase, evidenced by the higher values of speed found, with a maximal value of 2.1 $m.s^{-1}$ at the inlet. The analysis of turbulent kinetic energy (Figure 4C) also indicates an improvement in mixing when compared to Case 1, but still presenting zones of low mixing in the top portion.

The results for the simulation of Case 3, which has the highest recycle flow rate equal to 0.003 $m^3.s^{-1}$, are presented in Figure 5. By doubling the initial flow rate, the velocity mixing inside the reactor also increases, with a maximal value of 2.83 $m.s^{-1}$ (Figure 5A). The flow inside the reactor remains characterized by the presence of large vortices and the absence of preferential paths, reproducing the behavior observed in the previous cases (Figure 5B). However, there are higher values of the turbulent kinetic energy in the top portion of the reactor, which indicates an optimization of the mixture (Figure 5C). It can also be noted in Figure 5C that the reactor is fully turbulent, and thus there are no "dead zones" in which the phases are not mixed. This indicates that the flow rate considered in this case (0.003 $m^3.s^{-1}$) is sufficient to provide an efficient operation of the bioreactor.

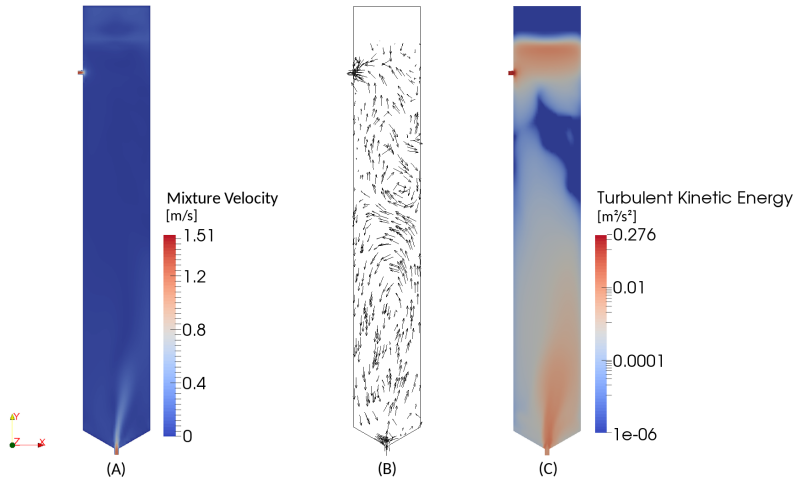

Figure 3: Case 1: (A) mixture velocity; (B) velocity vectors; (C) turbulent kinetic energy.

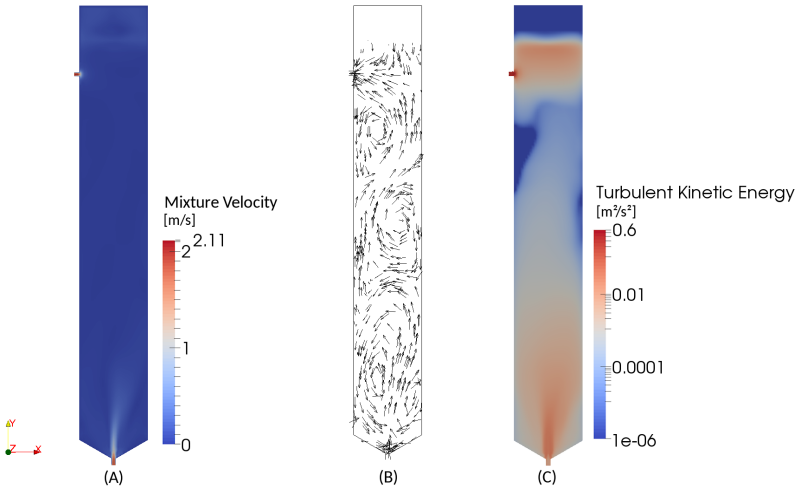

Figure 4: Case 2: (A) mixture velocity; (B) velocity vectors; (C) turbulent kinetic energy.

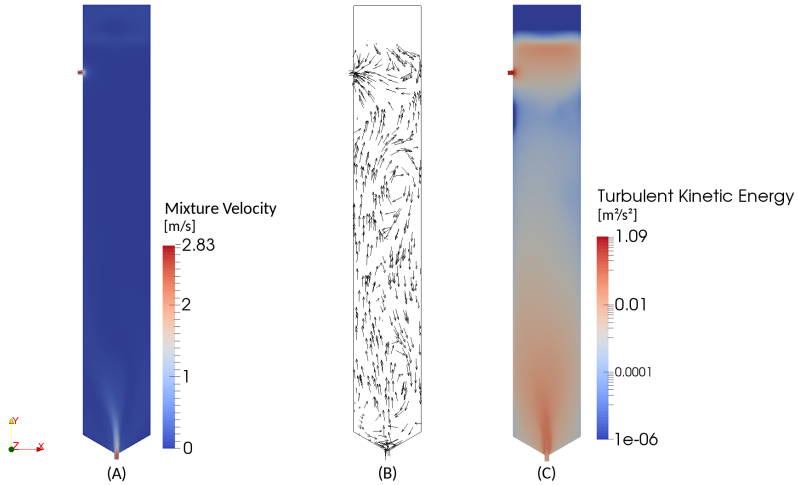

Figure 5: Case 3: (A) mixture velocity; (B) velocity vectors; (C) turbulent kinetic energy.

According to Nurtono *et al*. (2012), the maximal shear stress recommended in bioreactors is 0.66808 $N.m^{-2}$. Above this limit, there may be a disruption of the flocs that serve as support for the microbial activity. Figure 6 shows the values of maximal shear stress (Equation (13)) collected in a line along the diameter of the reactor, at 0.25 meters of height. These values are higher near the center, due to the inlet stream, and also near the walls of the bioreactor. It is observed that the highest flow rate provided larger values of shear stress, but they are below the given threshold. The maximal values were observed in the regions close to the recycling pipes, being equal to 0.531, 0.635 and 0.846 $N.m^{-2}$ for Cases 1, 2 and 3, respectively (Figure 7). Thus, the highest flow rate considered can lead to degradation of the flocs, and an inefficient operation of the reactor.

The problem observed in Case 3, in which the values of shear stress are above the recommended threshold, can be solved using recycle pipes with larger diameters, resulting in lower maximal velocities. Thus, three new diameters, of 0.048, 0.06 and 0.08 m were tested for the highest flow rate evaluated (0.0030 $m^3.s^{-1}$). As can be seen in Figure 8A, using a diameter of 0.048 m for the recycling pipes causes a small reduction in the shear stress, but it is still above the limit of 0.66808 $N.m^{-2}$. Figures 8B and 8C show the maximal shear stress values obtained using diameters of 0.06 and 0.08 m, respectively. A significant reduction in shear stress was observed, with the maximal values below the limit proposed by Nurtono *et al.* (2012). The use of different inlet diameters alters the flow pattern inside the bioreactor, but retains high values of turbulent kinetic energy, without the presence of stagnant zones. Thus, the adoption of a diameter of 0.06 m for the recycling pipes, using the highest flow rate (0.0030 $m^3.s^{-1}$) considered, can lead to a significant increase in the mixture inside the reactor, without affect the form of the flocs, improving the efficiency of the reactor.

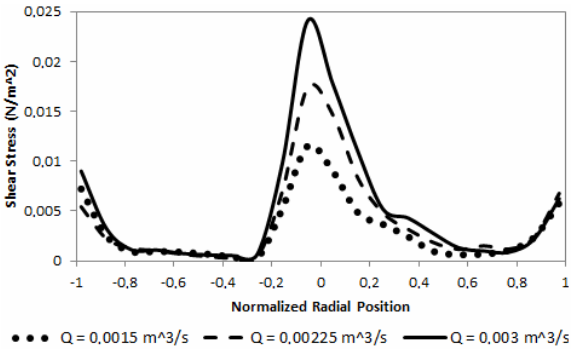

Figure 6: Maximal shear stress along the normalized radial position, at 0.25 m of height.

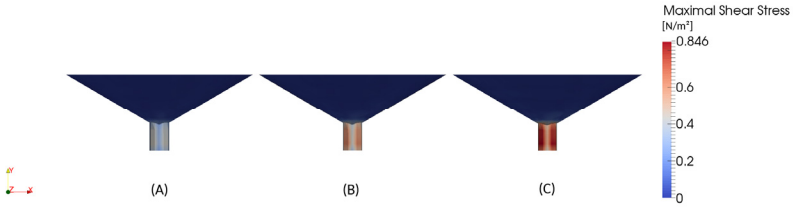

Figure 7: Maximal shear stress at the inlet pipe: (A) Case 1; (B) Case 2; (C) Case 3.

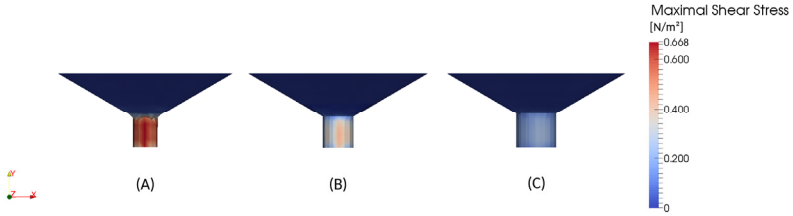

Figure 8: Maximal shear stress at the inlet pipe: (A) 0.048 m; (B) 0.06 m; (C) 0.08 m.

CONCLUSIONS

The fluid dynamics in an ASBR, operating with upward flow, was determined through numerical simulations. Three recycle flow rates were evaluated, and the results obtained for the velocity and turbulent kinetic energy indicate that the higher the flow considered, the greater is the mixture provided by the fluid within the reactor. Low values were observed for the maximal shear stress calculated inside the reactor. However, in the regions of higher velocities (close to the recycle pipeline) the values for the maximal shear stress observed were above the recommended range for Case 3.

This problem can be solved using recycle pipes of larger diameter, to maintain the integrity of the flocs in the case of higher flow rate, resulting in a better performance of the reactor. Results indicate that the best configuration for the reactor studied in this paper considers the use of larger pipes (0.06 m), with a higher flow rate (0.0030 $m^3.s^{-1}$).

It can also be concluded that CFD tools can be valuable to study the behavior of reactors. In the present study, different conditions were verified with numerical simulations, and their influence on the performance of the reactor was verified, leading to a possible optimization of the current process.

ACKNOWLEDGEMENTS

The authors are grateful to CENPES/Petrobras and FAPERGS for the financial support.

NOMENCLATURE

Latin Letters

C_μ, C_1, C_2	constant of the *k-epsilon* turbulence model	0.09, 1.44, 1.92
C_D	drag coefficient	(-)
d	bubble diameter	m
g	acceleration due to gravity	$m.s^{-2}$
I	unit tensor	(-)
k	turbulent kinetic energy	$m^2.s^{-2}$
L	length scale	m
L_e	eddy length scale	m
M	interphase momentum exchange term	$N.m^{-3}$
p	pressure	Pa
P	production of turbulent kinetic energy	$Pa.s^{-1}$
R	combined Reynolds (turbulent) and viscous stress	$m.s^{-1}$
Re	bubble Reynolds number	(-)
t	time	s
U	average velocity	$m.s^{-1}$
U_r	average relative velocity	$m.s^{-1}$

Greek Letters

α	volume fraction	(-)
ρ	density	$kg.m^{-3}$
υ	kinematic viscosity	$m^2.s^{-1}$
ε	turbulent dissipation energy	$m^2.s^{-3}$
τ	shear stress	$N.m^{-2}$
μ	dynamic viscosity	$kg.m^{-1}.s^{-1}$
σ_κ, σ_ε	constant of the κ-ε turbulence model	1.0, 0.76923
υ_l	laminar viscosity	$m^2.s^{-1}$
υ^t	eddy viscosity	$m^2.s^{-1}$

Subscripts

eff	Effective
g	gas phase
i	phase
l	liquid phase
T	transposed vector

REFERENCES

Arooj, M. F., Han, S. K., Kim, S. H., Kim, D. H., Shin, H. S., Sludge characteristics in anaerobic SBR system producing hydrogen gas. Water Research, 41, p. 1177-1184 (2007).

Bannari, R., Bannari, A., Selma, B., Proulx, P., Mass transfer and shear in an airlift bioreactor: Using a mathematical model to improve reactor design and performance. Chemical Engineering Science, 66, p. 2057-2067 (2011).

Bannari, R., Kerdouss, F., Selma, B., Bannari, A., Proulx, P., Three-dimensional mathematical modeling of dispersed two-phase flow using class method of population balance in bubble columns. Computer and Chemical Engineering, 32, p. 3224-3237 (2008).

Brito, A. G., Rodrigues, A. C., Melo, F. L., Feasibility of a pulse sequencing batch reactor with anaerobic aggregated biomass for the treatment of low strength wastewater. Water Science and Technology, 35, p. 193-198 (1997).

Chen, P., Sanyal, J., Dudukovic, M. P., Numerical simulation of bubble columns flows: Effect of different breakup and coalescence closures. Chemical Engineering Science, 60, p. 1085-1101 (2005).

Ding, J., Wang, X., Zhou, X. F., Ren, N. Q., Guo, W. Q., CFD optimization of continuous stirred-tank (CSTR) reactor for biohydrogen production. Bioresource Technology, 101, p. 7005-7013 (2010).

Fernandes, L., Kennedy, K. J., Ning, Z., Dynamic modeling of substrate degradation in sequencing batch anaerobic reactors (SBAR). Water Research, 27, p. 1619-1628 (1993).

Kim, D. H., Kim, S. H., Ko, I. B., Lee, C. Y., Shin, H. S., Start-up strategy for continuous fermentative hydrogen production: Early switchover from batch to continuous operation. International Journal of Hydrogen Energy, 33, p. 1532-1541 (2008).

Michelan, R., Zimmer, T. R., Rodrigues, J. A. D., Ratusznei, S. M., Moraes, D., Zaiat, M., Foresti, E., Effect of impeller type and mechanical agitation on the mass transfer and power consumption aspects of ASBR operation treating synthetic wastewater. Journal of Environmental Management, 90, p. 1357-1364 (2009).

Novaes, L. F., Saratt, B. L., Rodrigues, J. A. D., Ratusznei, S. M., Moraes, D., Ribeiro, R., Zaiat, M., Foresti, E., Effect of impeller type and agitation on the performance of pilot scale ASBR and AnSBR applied to sanitary wastewater treatment. Journal of Environmental Management, 91, p. 1647-1656 (2010).

Nurtono, T., Nirwana, W. O. C., Anwar, N., Kusdianto, Nia, S. M., Widjaja, A., Winardi, S., A computational fluid dynamics (CFD) study into a hydrodynamic factor that affects a bio-hydrogen production process in a stirred tank reactor. Procedia Engineering, 50, p. 232-245 (2012).

OpenFOAM, OpenFOAM User Guide (2013).

Pinheiro, D. M., Ratusznei, S. M., Rodrigues, J. A. D., Zaiat, M., Foresti, E., Fluidized ASBR treating synthetic wastewater: Effect of recirculation velocity. Chemical Engineering and Processing, 47, p. 184-191 (2008).

Pinho, S. C., Ratusznei, S. M., Rodrigues, J. A. D., Foresti, E., Zaiat, M., Feasibility of treating partially soluble wastewater in an aerobic sequencing batch biofilm reactor (AnSBBR) with mechanical stirring. Bioresource Technology, 96, p. 517-519 (2005).

Ren, T. T., Mu, Y., Liu, L., Li, X. Y., Yu, H. Q., Quantification of the shear stresses in a microbial granular sludge reactor. Water Research, 43, p. 4643-4651 (2009).

Rusche, H., Computational fluid dynamics of dispersed two-phase flows at high phase fraction. Ph.D. Thesis, Department of Mechanical Engineering, Imperial College of Science, Technology and Medicine, University of London, London, UK (2002).

Silva, M. K., D'Ávila M. K., Mori M., Study of the interfacial forces and turbulence models in a bubble column. Computers and Chemical Engineering, 44, p. 34-44 (2012).

Wang, X., Ding, J., Guo, W. Q., Ren, N. Q., Scale-up and optimization of biohydrogen production reactor from laboratory-scale to industrial-scale on the basis of computational fluid dynamics simulation. International Journal of Hydrogen Energy, 35, p. 10960-10966 (2010).

Weller, H. G., Derivation, modeling and solution of the conditionally averaged two-phase flow equations. Technical Report TR/HGW/02, Nabla Ltd. (2002).

Yu, L., Ma, J., Frear, C., Zhao, Q., Dillon, R., Li, X., Chen, S., Multiphase modeling of settling and suspension in anaerobic digester. Applied Energy, 111, p. 28-39 (2013).